

CsPbBr₃ and CH₃NH₃PbBr₃ Promote Visible-light

Photo-Reactivity

*Shankar Harisingh¹, Sujith Ramakrishnan¹ Michael Kulbak², Igal Levine², David Cahen²,
Bat-El Cohen¹, Lioz Etgar¹ and Micha Asscher^{*1}*

¹Institute of Chemistry, Edmund J. Safra Campus, Givat-Ram, The Hebrew University of
Jerusalem, 91904 Israel

²Department of Materials and Interfaces, Weizmann Institute of Science, Rehovot 76100,
Israel

* Corresponding author e-mail: micha.asscher@mail.huji.ac.il

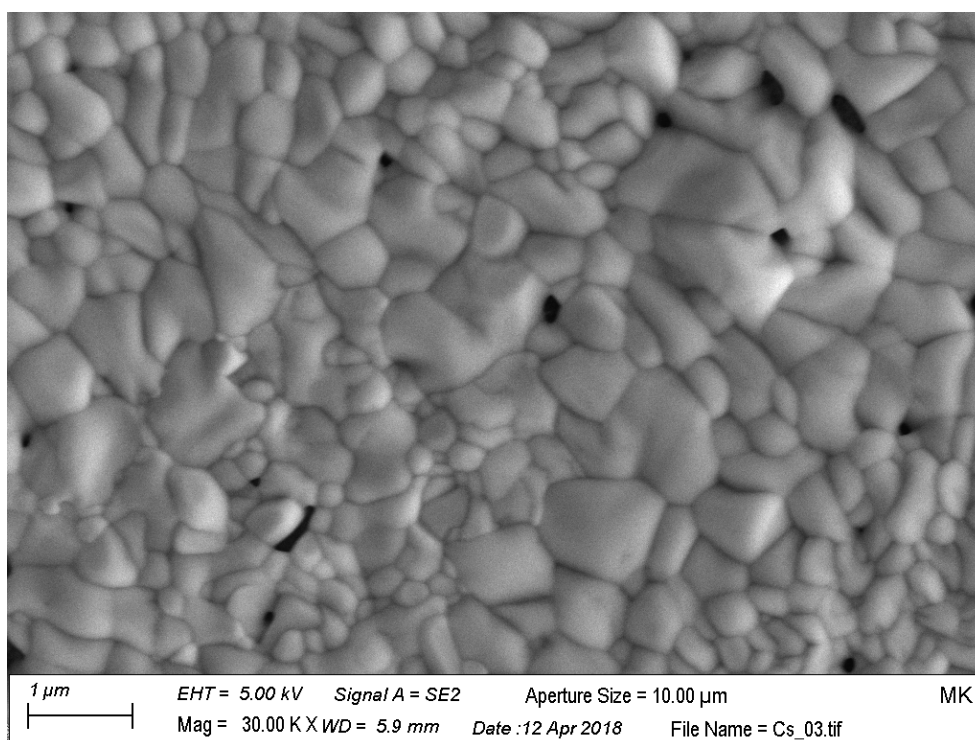
Keywords: Visible Light Surface-Photochemistry, Perovskites surfaces, Photoluminescence,
Electron Induced Luminescence

Supporting information:

Morphological and structural characterization results:

SEM, and XRD spectra of CsPbBr₃ and MAPbBr₃ substrates are shown in Figures S1 and S2 respectively. It is important to note that in order to minimize moisture and oxygen effects on our samples they were inserted into the UHV chamber as soon as we could. As a result, the data and images shown were taken on different samples that were prepared via identical procedures.

A)



B)

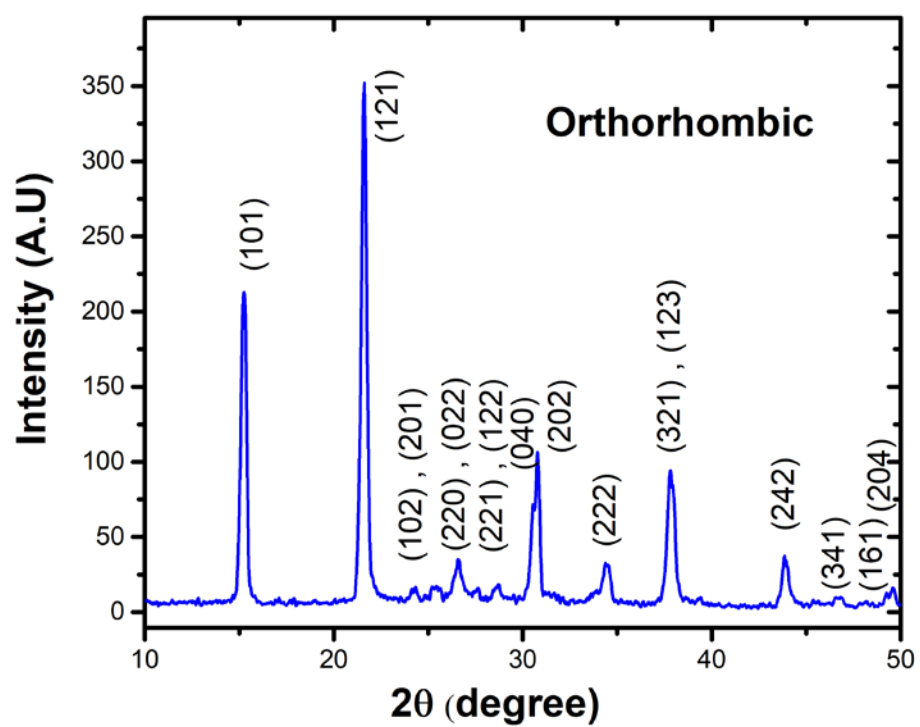
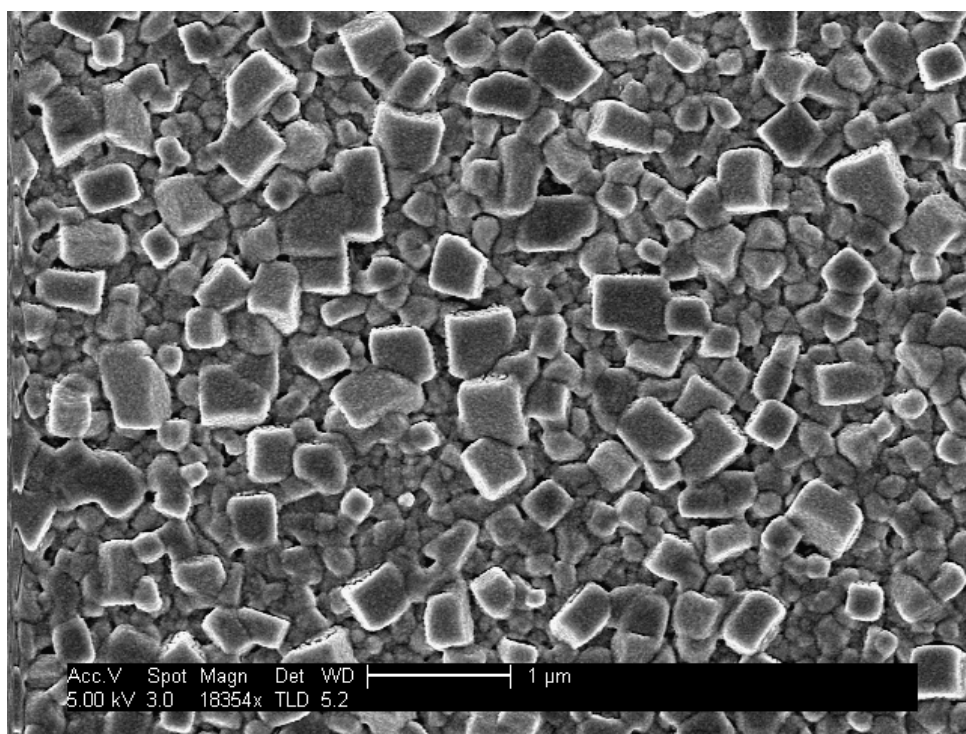


Figure S1: A) SEM image of a CsPbBr₃ sample prepared following the same procedure described in the experimental section B) XRD of the 300 nm thick CsPbBr₃ sample, revealing the expected orthorhombic phase of the material.

A)



B)

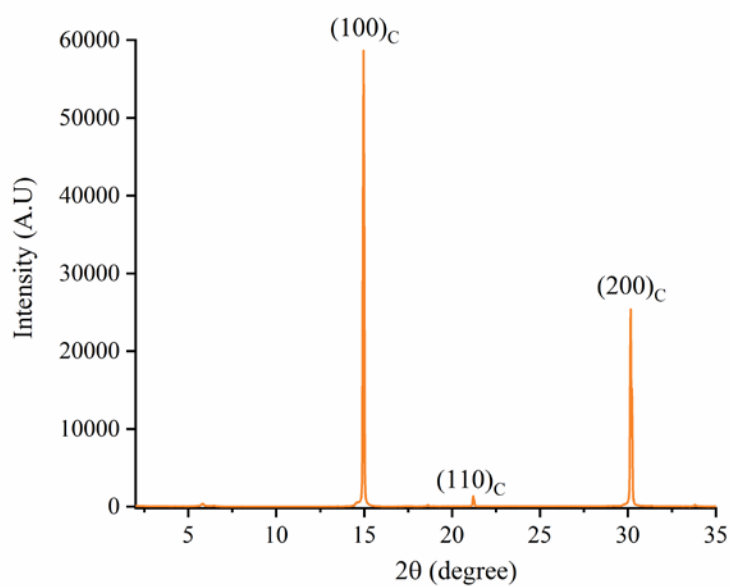


Figure S2: **A)** SEM image of a MAPbBr₃ sample prepared following the same procedure described in the experimental section **B)** XRD of the 400 nm thick MAPbBr₃ sample, revealing the expected cubic phase of the material.

TPD of Ethylchloride

Thermal desorption spectra of EC (mass 29) from CsPbBr₃/SiO₂/Si(100) and MAPbBr₃/SiO₂/Si(100) samples are shown in Fig.1(in the main text) and Fig.S3 respectively. In CsPbBr₃, two desorption peaks are observed: a high T peak (107 K) that saturates at EC exposures above 0.5 L and a low T peak (92 K) that does not reach saturation. The high temperature peak is attributed to the molecules directly adsorbed on the CsPbBr₃ surface (does not appear at all on the clean SiO₂ surfaces) and the low temperature peak to molecules desorbing from the multilayers accumulated on the perovskite surface. Similarly, in MAPbBr₃ two desorption peaks are observed: a high T peak at 110 K and a low T peak at 100 K, which are attributed to desorption from monolayer and multilayer, respectively. A gradual shift from the high T desorption at low coverage to the low T desorption at high coverage is due to repulsive interaction among neighbour molecules [see Ref. 17 in the main text]. On both perovskite surfaces, the desorption spectra suggest that one complete monolayer (1 ML) of EC adsorption takes place at the exposure of approximately 1.5 L. Hence, the definition of one monolayer (1.5 L= 1 ML) was kept throughout the photochemical experiments.

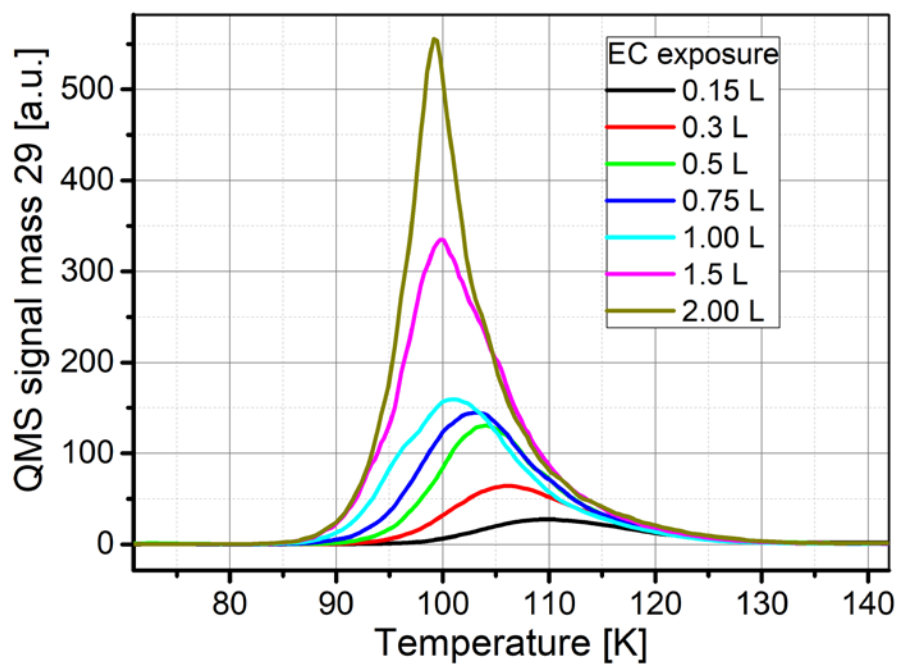


Figure S3. TPD spectra of EC adsorbed on MAPbBr₃/SiO₂/Si(100) sample at the indicated exposures in Langmuirs (L). Exposure values were corrected for ion gauge sensitivity factor. Heating rate was 1 K/sec.

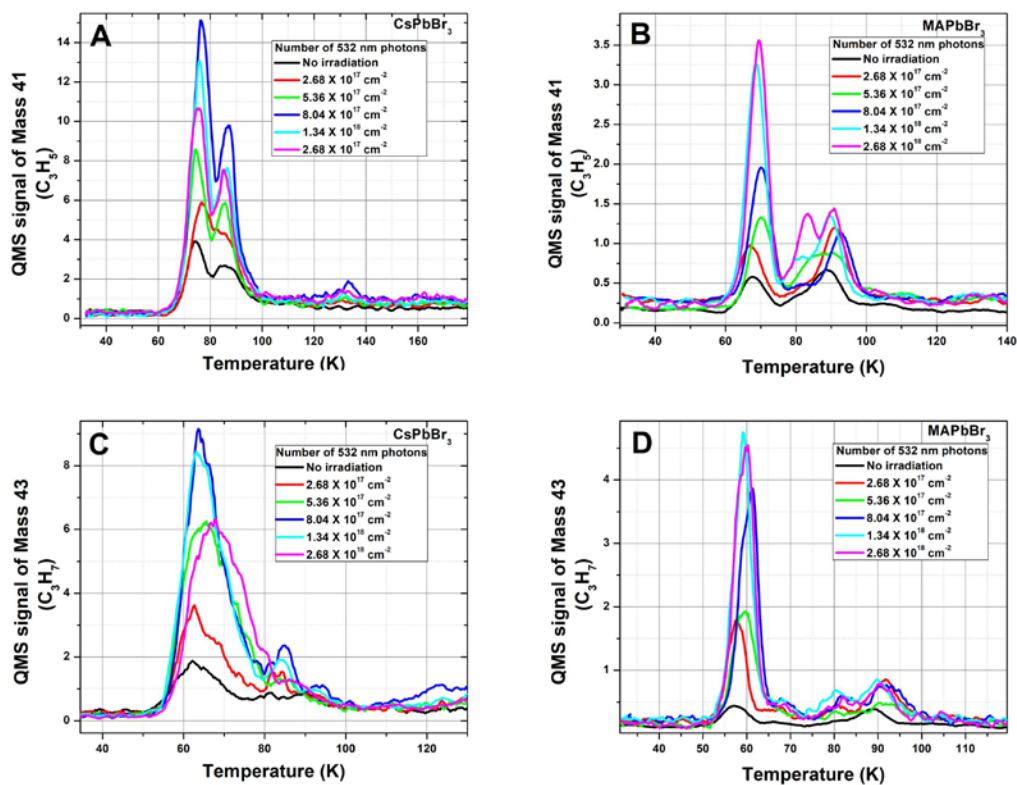


Figure S4: Post irradiation TPD spectra of the photo-product, (A) and (B) Allyl radical (mass-41, C₃H₅), (C) and (D) Propyl radical (mass-43, C₃H₇) at the indicated number of 532 nm photons striking CsPbBr₃ and MAPbBr₃ samples. The heating rate was 1 K/sec.

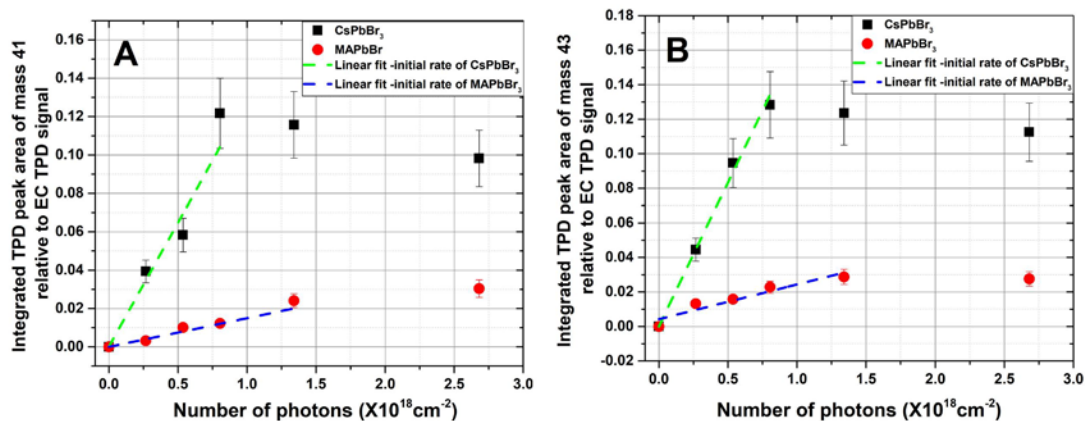


Figure S5: Integrated TPD peaks vs. visible (532 nm) light excitation of the photo products (A) Allyl radical (mass-41, C_3H_5) and (B) Propyl radical (mass-43, C_3H_7) (derived from Figs. S4) vs. the number of 532 nm photons striking the CsPbBr₃ and MAPbBr₃ perovskite samples. A linear fit for the initial growth was used for product molecules formation cross section determination.

See discussion in Fig. 3 of the main text of why the linear initial rate is used instead of an exponential expression. The formation cross sections on the two perovskite surfaces are summarized in Table 1 of the main text.

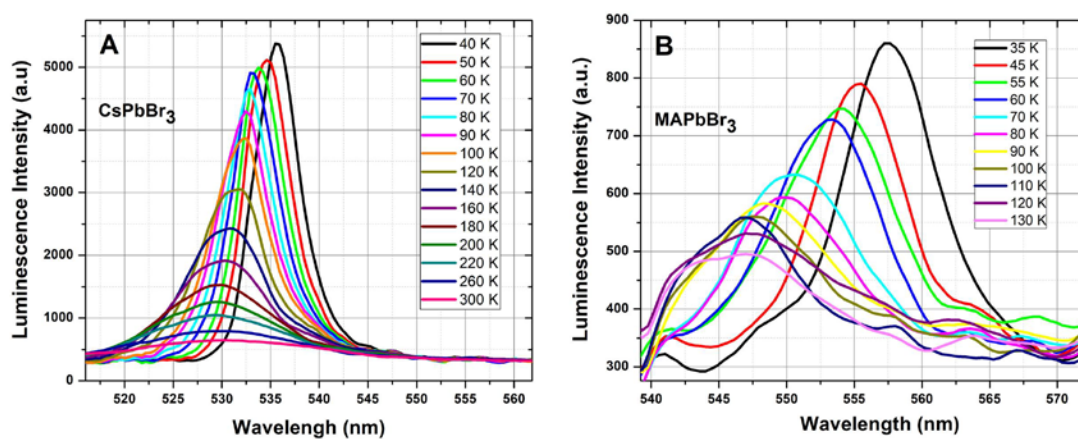


Figure S6. Photon-induced luminescence: PL spectra obtained while exciting the (A) CsPbBr₃ and (B) MAPbBr₃ by 355 nm laser at the indicated sample temperature between 40-300 K.

PL spectra of CsPbBr₃ are shown in Fig. S6A, following excitation by a pulsed (6 ns) 3rd harmonic emission from a Nd:YAG laser source, operating at a repetition rate of 10 Hz. The symmetrical shape of the PL peak confirms the negligible contribution from defects¹, which is consistent with the high conversion efficiency of light to electric energy in photovoltaic applications. As evident from Fig. S6A, the temperature dependence of the luminescent spectral peak position and intensity is different in the low and high temperature regions. The blue shift observed in the low temperature region (From 40 to 180K) is in contrast to the behaviour of typical semiconductors such as Si, Ge and GaAs for which the bandgap narrows with increasing temperature as a result of lattice dilation^{2,3}. Hence, the conventional empirical models (Varshni and Bose-Einstein) are no longer applicable for these types of materials. This unusual behaviour is usually attributed to the competition between lattice thermal expansion and electron-phonon coupling and was extensively discussed in the literature⁴⁻⁶. Such blue shift is also observed in CsPbBr₃ nanowires⁴, in PbSe, PbTe⁵ and CsSnI₃⁶.

Fig. S6B reveals the temperature-dependent PL spectra of MAPbBr₃. Even though both halide perovskite films were excited by the same laser power density (1 mJ/cm² per pulse), the luminescence peak intensity of MAPbBr₃ is significantly lower than that of CsPbBr₃ due to the thermal quenching. The temperature-dependent PL spectra of MAPbBr₃ show two main characteristics: (i) similar to CsPbBr₃, as the temperature increases from 35 to 100 K, a significant blue shift is noticed. The PL peak gradually shifts from 557.6 nm to 546.5 nm, while the PL intensity drops. The low temperature peak can be ascribed to lowest energy excitons⁷; (ii) as the temperature is further increased from 100 to 130 K the PL peak is at a stable (optical) position and gradually splits into two peaks. The asymmetric behaviour of these two newly evolved peaks

appeared at 120 K can be attributed to the surface states, denoted as bound excitons^{8,9}. Poglitsch et al¹⁰ reported a phase transition in MAPbBr₃ single crystals from the orthorhombic to tetragonal phase at 145 K. There are a few other reports, in which this phase transition behaviour was not observed for CVD grown MAPbBr₃ nanowires and for MAPbBr₃ thin film samples^{8,9}. But, in our PL studies, when the temperature is increased above 130 K the PL signal disappeared completely due to the significant thermal quenching effect. Hence, it was not possible to confirm the presence of the PL peak corresponding to the phase transition, as reported for the bulk crystals. However, the phase transition behaviour is not that significant to the current study. Since our main objective to study the PL was the search for the presence or absence of defects, the results have led us to conclude that there is a defect site (observed at 120 K) in MAPbBr₃ and this defect is expected to have an influence on the photo-reactivity of the MAPbBr₃ films, namely to reduce the photochemical cross-section of the various photo-products.

The e-beam induced luminescence (EBIL) was studied with different coverage values of EC by varying the exposure (0 to 3 L) of EC on the CsPbBr₃ and the results are consistent with the TPD data shown in Figures 1 and S3.

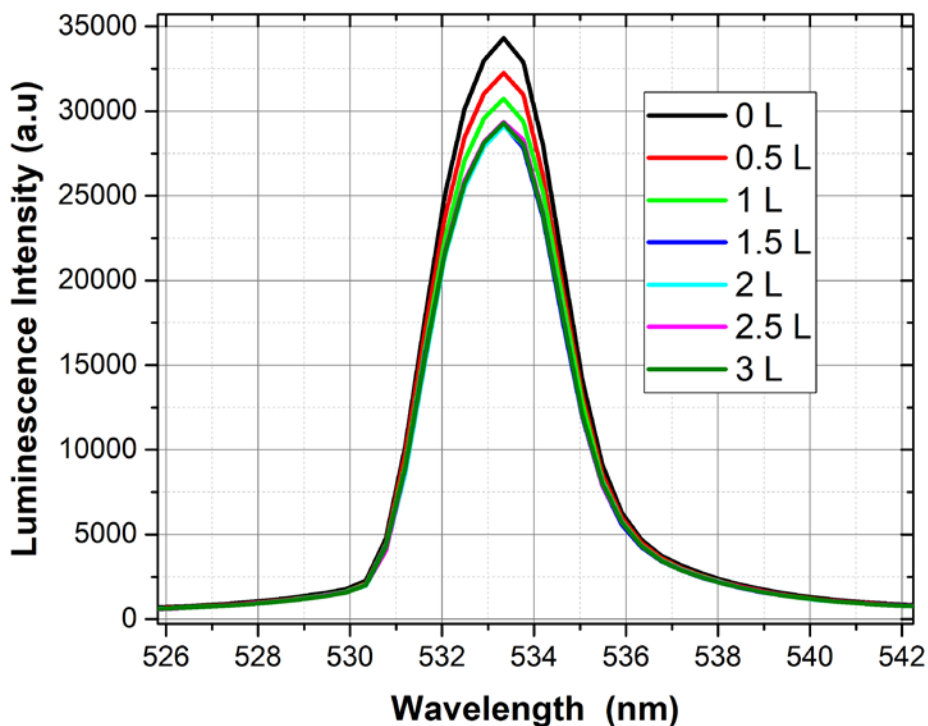


Figure S7. Electron beam-induced Luminescence spectra of the CsPbBr₃ substrate with different exposures of EC (in Langmuir units) at 35 K.

EBIL with different exposures of EC is shown in Fig. S7. The luminescence signal is found to slightly decrease (by 15%) with increasing the EC exposure from zero to 1.5 L exposure (1 ML coverage) and then it stays at a constant luminescence intensity beyond 1.5 L. This is because the luminescence signal is affected only by EC molecules, adsorbed directly on the CsPbBr₃ surface (i.e. monolayer) while the EC molecules on top of other EC molecules (2nd layer and above), do not have direct interaction with the CsPbBr₃ substrate; therefore, these molecules do not contribute to the luminescence signal quenching.

References:

1. K. Wei, Z. Xu, R. Chen, X. Zheng, X. Cheng, T. Jiang, Temperature-dependent excitonic photoluminescence excited by two-photon absorption in perovskite CsPbBr₃ quantum dots. *Opt. Lett.* 2016, **41**, 3821-3824.
2. J. Bardeen, W. Shockley, Deformation Potentials and Mobilities in Non-Polar Crystals. *Phys. Rev.* 1950, **80**, 72-80.
3. Y. P. Varshni, Temperature dependence of the energy gap in semiconductors. *Physica* 1967, **34**, 149-154.
4. D. Zhang, S. W. Eaton, Y. Yu, L. Dou, P. Yang, Solution-Phase Synthesis of Cesium Lead Halide Perovskite Nanowires. *J. Am. Chem. Soc.* 2015, **137**, 9230-9233.
5. M. Baleva, T. Georgiev, G. Lashkarev, On the temperature dependence of the energy gap in PbSe and PbTe. *J. Phys. Condens. Matter* 1990, **2**, 2935.
6. C. Yu, *et al.* Temperature dependence of the band gap of perovskite semiconductor compound CsSnI₃. *J. Appl. Phys.* 2011, **110**, 063526.
7. K. Tanaka, T. Takahashi, T. Ban, T. Kondo, K. Uchida, N. Miura, Comparative study on the excitons in lead-halide-based perovskite-type crystals CH₃NH₃PbBr₃ CH₃NH₃PbI₃. *Solid State Commun.* 2003, **127**, 619-623.
8. J. Dai, H. Zheng, C. Zhu, J. Lu, C. Xu, Comparative investigation on temperature-dependent photoluminescence of CH₃NH₃PbBr₃ and CH(NH₂)₂PbBr₃ microstructures. *J. Mater. Chem. C*, 2016, **4**, 4408-4413.
9. D. Priante, *et al.* The recombination mechanisms leading to amplified spontaneous emission at the true-green wavelength in CH₃NH₃PbBr₃ perovskites. *Appl. Phys. Lett.* 2015, **106**, 081902.
10. A. Poglitsch, D. Weber, Dynamic disorder in methylammoniumtrihalogenoplumbates (II) observed by millimeter-wave spectroscopy. *J. Chem. Phys.* 1987, **87**, 6373-6378.